A Journal of the Gesellschaft Deutscher Chemiker

Angewandte International Edition GDCh Chemie

www.angewandte.org

Accepted Article

Title: Azobispyrazole family as photoswitches combining (near-) quantitative bidirectional isomerization and widely tunable thermal half-lives from hours to years

Authors: Yixin He, Zhichun Shangguan, Zhao-Yang Zhang, Mingchen Xie, Chunyang Yu, and Tao Li

To be cited as: *Angew. Chem. Int. Ed.* 10.1002/anie.202103705

Link to VoR: https://doi.org/10.1002/anie.202103705

WILEY-VCH

10.1002/anie.202103705

WILEY-VCH

Azobispyrazole family as photoswitches combining (near-) quantitative bidirectional isomerization and widely tunable thermal half-lives from hours to years

Yixin He,[a] Zhichun Shangguan,[a] Zhao-Yang Zhang,*[a] Mingchen Xie,[a] Chunyang Yu,[a] and Tao Li*[a]

[a] Y. He, Z. Shangguan, Dr. Z. Y. Zhang,* M. Xie, Prof. C. Yu, and Prof. T. Li*
School of Chemistry and Chemical Engineering, Frontiers Science Center for Transformative Molecules, Shanghai Key Laboratory of Electrical Insulation and Thermal Aging
Shanghai Jiao Tong University
Shanghai 200240, China
E-mail: litao1983@sjtu.edu.cn; zy_zhang@sjtu.edu.cn

Supporting information for this article is given via a link at the end of the document.

Abstract: Azobenzenes are classical molecular photoswitches that have received widespread application. In recent endeavors of molecular design, replacing one or both phenyl rings by heteroaromatic ones is emerging as a strategy to expand the molecular diversity and access improved photoswitch properties. Many mono-heteroaryl azo molecules with unique structure/properties have been developed, but the potential of bis-heteroaryl architecture is far from exploited. Here we report a family of azobispyrazoles, which combine (near-)quantitative bidirectional photoconversion and widely tunable *Z*-isomer thermal half-lives from hours to years. The two five-membered rings remarkably weaken the intramolecular steric hindrance, providing new possibilities for the engineering geometric and electronic structure of azo photoswitches. Azobispyrazoles generally exhibit twisted *Z*-isomers that facilitate complete *Z*→*E* photoisomerization, and their thermal stability can be adjusted independently of geometric shape, overcoming the conflict between effective photoconversion (favored by twisted shape) and *Z*-isomer stability (favored by T shape) encountered by mono-heteroaryl azo switches.

Introduction

Molecular photoswitches, which can be reversibly interconverted between different states by light irradiations, have inspired intensive efforts in developing light-responsive systems for diverse applications.[1] Azobenzenes are the most widely used photoswitches and play dominating roles in many areas, such as photomechanical actuation of soft materials,[2] photopharmacological modulation of physiological functions,[3] and photochemical solar thermal energy storage.[4] For azo photoswitches, probably the foremost factor determining their quality is the $E \leftrightarrows Z$ photoisomerization yields in both directions. In general, quantitative bidirectionality is highly desirable, since incomplete photoconversion in any direction will compromise the capability of photoswitching. Another essential property is the thermal stability of metastable isomers (*Z*-forms, in general), which spontaneously relax back to the thermodynamically stable states. The suitable thermal back-isomerization kinetics, represented by half-lives $t_{1/2}$ (values are at 25 °C hereinafter, if not specified), depends on the application of interest. For example, $t_{1/2}$ ranging from seconds to hours can match the timescales of various biological events,[5] while ultralong $t_{1/2}$ of months to years are advantageous to information and energy storage.[4a,6]

Azobenzene (Ph-N=N-Ph) itself is a highly adaptable molecular architecture because of its numerous structural modification possibilities. Since the discovery of azobenzene photoisomerization in 1937,[7] introducing substituent groups to phenyl rings has produced a vast number of azobenzene derivatives.[8] Important progress includes *ortho*-substitutions based visible-light-switchable azobenzenes.[9] In recent endeavors of molecular design, replacing one or both phenyl rings by heteroaromatic ones has attracted increasing attention.[10] The diversity of heterocycles and their distinct nature from benzene provide tremendous opportunities to regulate the performance of azo switches. Six-membered rings such as pyridine[11] and pyrimidine[12] afforded heteroaryl azo switches in which coordination interactions and hydrogen bonding could be utilized. Significantly, mono-heteroaryl azo molecules (Ph-N=N-Het) based on five-membered rings (imidazole,[13] pyrazole,[14] pyrrole,[14] thiophene,[15] isoxazole,[16] etc.) showed some unusual features. Herges group[13b] and Fuchter group[14a] reported that *Z*-isomers of phenylazoimidazoles and phenylazopyrazoles could adopt a T-shaped geometry (where the phenyl ring was orthogonal to the azo-heterocycle moiety) not accessible by azobenzenes. Herges et al[13b] disclosed that such T geometry could enlarge the difference in conjugation degree between *E* and *Z* isomers and thus their π-π* absorption bands were well separated, enabling complete *E*→*Z* photoisomerization. A later systematic study by Fuchter and Contreras-García et al[14b] revealed that the T geometry was crucial for high *Z*-isomer stability ($t_{1/2}$ up to 1000 days) but detrimental to *Z*→*E* photoconversion (due to the weak n-π* absorbance of *Z*-isomers). Structural modifications that twisted the conformation could improve the photoisomerization yields, which, however, shortened their *Z*-isomer $t_{1/2}$.[14b,17] Phenylazothiophenes also allowed T-shaped *Z*-isomers; they similarly displayed complete *E*→*Z* and unfavorable Z→*E* photoconversion, while their $t_{1/2}$ (20 °C) were at the timescale of hours or less.[15] Azo switches bearing a benzoheterocycle such as quinoline,[12b] indole,[18] indazole,[19] and purine[20] were also

reported. Their extended π system generally led to bathochromic shifts of π-π* absorption bands and accelerated back relaxation with $t_{1/2}$ from nanoseconds to days. In spite of the important progress on mono-heteroaryl azo switches, a great challenge remains on how to achieve quantitative bidirectional photoconversion and, at the same time, tune their $t_{1/2}$ from short to very long.

Bis-heteroaryl azo architecture (Het-N=N-Het) can further expand the molecular diversity and offers a probably more progressive way in tailoring the geometric and electronic structure, which, however, has not received sufficient attention. Fuchter group[21] designed and synthesized azobis(2-imidazole), a visible-light-responsive azo switch with 90% and ~100% conversions for *E*→*Z* and *Z*→*E* directions, respectively. Its *Z*-isomer adopted a twisted conformation and $t_{1/2}$ was only 16 s. Very recently, Beves et al[22] studied some azobisbenzazoles bearing benzimidazoles, benzoxazole or benzothiazoles, which showed 73 – 84% *E*→*Z* conversions under visible light. Notably, azobisbenzimidazole obtained a $t_{1/2}$ of 520 s, which was among the longest known for visible-light-switchable azoheteroarenes.[22] Azobisthiophenes were shown to be different from phenylazothiophenes in that their *Z*-isomers were also twisted and $t_{1/2}$ were up to 38 days (22 °C), yet their photoisomerization yields remain to be determined.[23] By combining electron-rich (thienyl)pyrrole/bithiophene and electron-deficient (benzo)thiazole, a series of push-pull bis-heteroaryl azo switches were constructed, which were responsive to visible light and their *Z*-isomer $t_{1/2}$ ranged from milliseconds to seconds.[24] In view of the very limited types of bis-heteroaryl azo switches reported so far and their limitations on bidirectional photoconversion and/or *Z*-isomer stability, the potential of Het-N=N-Het architecture is far from exploited, calling for the development of new molecular systems.

Here we present a family of azobispyrazoles as new photoswitches, as shown in Figure 1, all of which show excellent bidirectional photoconversion, and their *Z*-isomer $t_{1/2}$ can be broadly tuned from hours to years by changing the linking position between the azo group and pyrazole rings. As revealed by systematic experimental and theoretical investigations, azobispyrazoles show different structure-property relationships from mono-heteroaryl azo switches. In particular, their twisted *Z*-isomers can accommodate a wide range of $t_{1/2}$ timescales including hours, days, weeks, months, and years. Therefore, our work demonstrates the great potential of Het-N=N-Het architecture in molecular design, performance improvement, and broad applications of azo photoswitches.

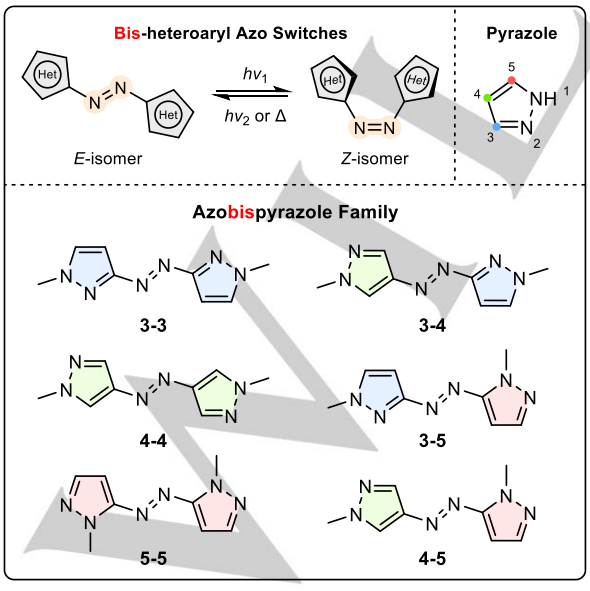

Figure 1. Molecular design of azobispyrazole family (*N*-methylation is necessary to prevent the azo-hydrazone or annular tautomerization).

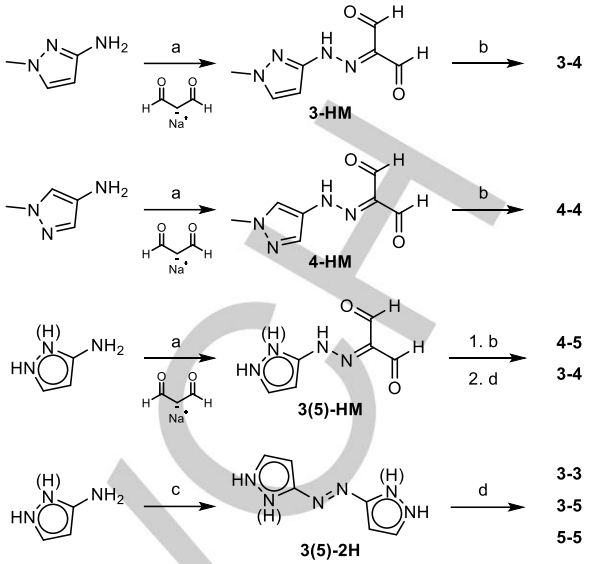

Scheme 1. Synthesis routes of azobispyrazoles. Reagent and conditions. (a) AcOH, concentrated HCl, aqueous $NaNO_2$, 0 °C, then aqueous KOAc, **MDA-Na**, 0 – 5 °C, 51 – 54%; (b) Methylhydrazine sulfate, KOAc, EtOH, refluxed, 65 – 80%; (c) MnO_2, $CHCl_3$, 80 °C, 25%; (d) CH_3I, Cs_2CO_3, DMF, room temperature, 83 – 85%.

Results and Discussion

Molecular Design and Synthesis

By bridging two pyrazole rings with an azo group at C3, C4, or C5 positions, a family of six azobispyrazoles can be formulated, including three symmetrical members (**3-3**, **4-4**, and **5-5**) and three asymmetrical members (**3-4**, **3-5**, and **4-5**), as shown in Figure 1. Because of the distinct nature of the three kinds of carbons on pyrazole, variations in linkage pattern can regulate the molecular geometries and electronic structure of the whole system, which is expected to have a significant effect on their photoswitch properties.

Synthesis routes of azobispyrazole family were shown in Scheme 1. In previous studies, phenylazopyrazoles containing 3,5-dimethylated 4-pyrazole were synthesized by diazo couplings between phenylamine and acetylacetone with subsequent ring formation.[14a,25] Inspired by this method, we first attempted to prepare our azobispyrazoles containing methyl-free 4-pyrazole (**3-4**, **4-4**, and **4-5**) using pyrazolylamines and malonaldehyde that was generated from *in situ* hydrolysis. However, the yield of diazo coupling step was uncontrollable (5 – 50% in different trials) since the malonaldehyde was prone to polymerize in solution during the hydrolytic process. Therefore, we employed malonaldehyde sodium salt (**MDA-Na**), which can

be isolated in pure solids and is stable over weeks in dry atmosphere.[26] In this way, pyrazolyl hydrazone intermediates (**3-HM**, **4-HM**, and **3(5)-HM**) were obtained in reproducible yields of ~50%. Further reactions with methylhydrazine sulfate constructed the 4-pyrazole rings, forming the other moieties of azobispyrazoles. The other three members (**3-3**, **3-5**, and **5-5**) were prepared in one pot through oxidation coupling of 1*H*-pyrazol-3(5)-amine[27,28] and subsequent *N*-methylation at two selectable positions, benefitting from the annular tautomerism of 1*H*-pyrazole. **3-3** and **5-5** were also obtained by electrochemical synthesis in previous work.[29] The single-crystal structures of all six members have been determined by X-ray crystallographic analysis (see Section 4 in the Supporting Information, SI). We note that photochromic properties of **3(5)-2H** were recently studied by König group.[28] It formed an equilibrium mixture of different tautomers (due to annular or azo-hydrazone tautomerism), and the preferred tautomeric form depended on solvent environment, which remarkably affected molecular property including photoisomerization yields and *Z*-state stability.

Photoisomerization and Electronic Transition Analysis

The photoisomerization properties of azobispyrazoles were studied by UV-Vis absorption spectroscopy in acetonitrile solution. As shown in Figure 2, the *E*-isomers exhibited strong π-π* absorption bands in 300 – 400 nm region (ε_{max} = 18 – 27×10^3 M^{-1} cm^{-1}), and the peak positions varied with the linkage pattern. As detailed in Table 1 and Figure 2, the π-π* λ_{max} red-shifted from 325 – 327 nm (**3-3**, **3-4**, and **4-4**) to 342 nm (**3-5**

Table 1. Spectroscopic data, $E \leftrightarrows Z$ photoisomerization and thermal $Z \rightarrow E$ isomerization properties of azobispyrazole family.

	E-isomer[a]		*Z*-isomer[a]		Photoconversion[b]		Quantum yield[c]		Thermal $Z \rightarrow E$ isomerization				
	π-π* λ_{max} (nm)	n-π* λ_{max} (nm)	π-π* λ_{max} (nm)	n-π* λ_{max} (nm)	$E \rightarrow Z$ (%)	$Z \rightarrow E$ (%)	$E \rightarrow Z$	$Z \rightarrow E$	$t_{1/2}$ (d)	$\Delta G^{\ddagger}_{exp}$[k] (kJ mol^{-1})	$\Delta H^{\ddagger}_{exp}$[k] (kJ mol^{-1})	$\Delta S^{\ddagger}_{exp}$[k] (J mol^{-1} K^{-1})	$\Delta G^{\ddagger}_{calc}$[l] (kJ mol^{-1})
4-4	327	~395	277	420	98[d]	99 / ~100[g]	0.43[d]	0.76[h]	681[i]	118.3	105.6	-42.5	109.2
3-4	326	~394	277	414	97[d]	97 / 99[g]	0.32[d]	0.47[h]	623[i]	118.0	104.2	-46.4	108.0
3-3	325	400	277	430	97[d]	98 / 99[g]	0.34[d]	0.62[h]	72[i]	112.7	96.1	-55.7	103.9
4-5	342	–	285	430	97[e]	98 / 99[g]	0.47[e]	0.72[h]	25[i]	110.1	95.4	-49.4	100.9
3-5	342	~413	293	441	97[e]	98 / 99[g]	0.42[e]	0.56[h]	6[i] (7[j])	106.5	91.1	-51.4	99.3
5-5	356	–	313	454	94[f]	99 / ~100[g]	0.36[e]	0.49[h]	0.3[i] (0.3[j])	99.1	86.2	-43.3	91.4

[a] The λ_{max} were taken from UV-Vis absorption spectra measured in MeCN (4×10^{-5} M). [b] The isomer composition were obtained through integrating the peak areas of ^{1}H NMR spectra measured in CD_3CN solution (see Section 2.2 in SI). [c] The quantum yields were determined in MeCN, and the errors were within ± 0.02 (see Section 2.4 in SI). [d–h] The samples were irradiated with lights of [d] 350 nm, [e] 365 nm, [f] 370 nm, [g] 523 / 530–550 nm, and [h] 470 nm. [i] Values at 25 °C in DMSO, extrapolated from the experimental kinetics data at elevated temperatures using Arrhenius equation (see Section 3 in SI). [j] Values at 25 °C measured in MeCN. [k] Values at 25 °C in DMSO, calculated through Eyring plot based on the experimental kinetics data (see Section 3 in SI). [l] Values at 25 °C in DMSO, computed at B2PLYP-D3(BJ)/def2-TZVP//PBE0-D3(BJ)/6-31G** level of theory with solvation free energies at M05-2X/6-31G* level, considering the weights of all possible pathways (Table S21).

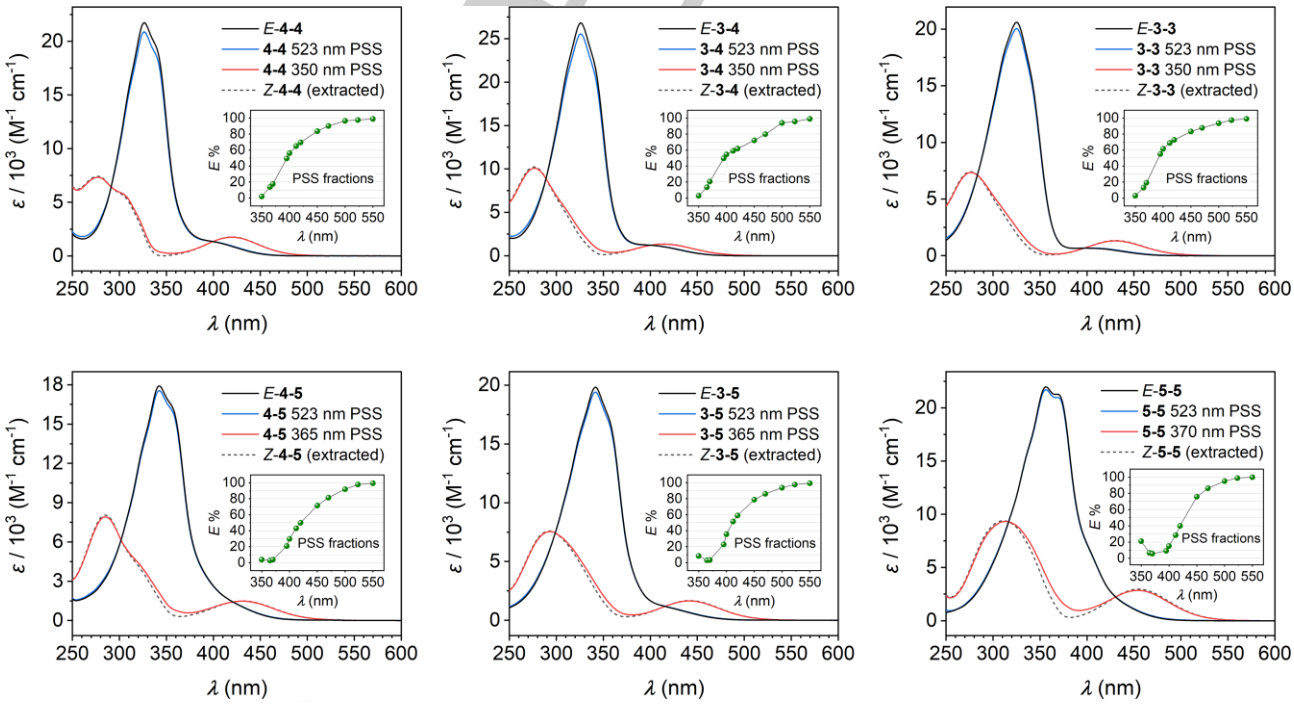

Figure 2. UV-Vis absorption spectra with molar extinction coefficients of azobispyrazoles in MeCN (see the zoomed-in spectra of n-π* regions in Figure S2). Insets show the *E*-isomer contents at 350 – 550 nm photostationary states (see tabulated results in Table S2 and corresponding spectra in Figure S9).

and **4-5**) and further to 356 nm (**5-5**). In all cases, irradiating the *E*-isomers at π-π* bands with appropriate light sources (350/365/370 nm) resulted in almost complete conversions (94 – 98%) to *Z*-isomers, benefitting from the overwhelming absorbance of *E* over *Z* isomers at the excited wavelengths. These *Z*-isomers displayed more evident n-π* absorption bands in visible range than *E*-isomers, and exciting the n-π* transition at band tails using green lights (523 nm or longer wavelengths) could induce quantitative backward isomerization for all azobispyrazole members. In contrast, the mono-pyrazolyl azo switches (phenylazopyrazoles), regardless of the linkage pattern, suffered from heavy overlapping of the n-π* bands between two isomers, which restricted the yields/efficiency of their *Z*→*E* photoisomerization,[14] and thus structural modification by substitution at the phenyl/pyrazole ring was necessary to improve the performance.[14a,17] Moreover, **5-5** could be used as a visible-light-induced photoswitch, which provided 85% *E*→*Z* and ~100% *Z*→*E* conversions by 400 and 530 – 550 nm light irradiations, respectively (Figure 2, inset and Table S2).

Azobispyrazoles could be soluble in various solvents even in water (slightly soluble), therefore we examined the solvent effect on UV-Vis absorption spectra using five solvents (*n*-hexane, EtOH, MeCN, DMSO, water). As shown in Table S5, the π-π* bands of *E*-isomers generally red-shifted with the increase of solvent polarity, while water induced blue shifts for the 5-pyrazole series (**3-5**, **4-5**, and **5-5**). The n-π* λ_{max} of *Z*-isomers did not show obvious variation with solvent polarity except that water induced blue shifts again. On the whole, solvents had a limited effect on spectral characteristics and did not apparently affect *E* ⇆ *Z* photoisomerization yields (see the UV-Vis spectra in different solvents in Figures S12 – S15).

We then determined the photoisomerization quantum yields of azobispyrazoles in acetonitrile solution (see results in Table 1 and S4). For *E*→*Z* (π-π* excitation) and *Z*→*E* (n-π* excitation) isomerizations, the quantum yields were 0.32 – 0.47 and 0.47 – 0.76, respectively, which were generally higher than those of azobenzene (0.10 – 0.15 and 0.41 – 0.58).[8a] Quantum yield results of heteroaryl azo were very limited in literature, but the advantage of Ph-N=N-Het molecules over azobenzene was also shown by azoimidazoles,[13a] azopyrrole,[14a] azopyrazoles,[14a,28] and azothiophene.[15a] More experimental and theoretical efforts are needed to gain a clear understanding that how heteroaryl substitution makes the photochemical processes more productive.

In order to reveal the relationship between molecular structures and electronic transition characteristics, density functional theory (DFT) and time-dependent DFT studies were carried out for all possible conformers of azobispyrazoles (see Section 5 in SI). For the *E*-isomers, the π-π* absorption band (S_0→S_2 excitation) corresponded to HOMO→LUMO transition (Figure 3a). The calculated λ_{max} agreed well with the experimental values, which red-shifted with the reduction of H–L gaps. This reflected the dependence of π-conjugation degree on the linkage pattern. According to the electron-donating conjugative effect from pyrrole-type N lone pair, the 5-pyrazole forms a "complete" conjugation pathway with the azo group while those from 4- and 3-pyrazole are only "partial".[14b] As a result, the molecular architecture bearing more 5-pyrazole units showed larger π-conjugation extension in pyrazole-azo-pyrazole system, making the π-π* λ_{max} follow the order of **5-5** > **3**(**4**)**-5** > **3**(**4**)**-3**(**4**). The n-π* band (S_0→S_1 excitation) of *E*-isomers corresponded to HOMO-1→LUMO transition (Figure 3a). It appeared that n-π* transitions require less excitation energies than π-π* but with larger gaps (H-1–L gaps vs. H–L gaps). This discrepancy, which was also found in other azoheteroarenes,[13a,14b,16,17c,18a] can be ascribed to the difference in exciton binding energies.[30]

For *Z*-isomers, the frontier molecular orbital (FMO) theory could not well describe the nature of electronic excitations, since the frontier occupied molecular orbitals mixed n and π composition and each transition was contributed by multiple sets of orbitals. Therefore, the natural transition orbital (NTO) analysis[31,32] was performed, and we found that the S_0→S_1 and S_0→S_2 excitations could be almost identified as n-π* and π-π* transitions, respectively (Figure 3b).

All *E*-isomers of azobispyrazoles showed a planar geometry and their n-π* transitions were symmetry-forbidden with negligible oscillator strength (*f*) of 0.0000 – 0.0001 (Tables S22 – S24). By contrast, the *Z*-isomers generally adopt a twisted geometry where two rings and azo group formed three dihedral angles φ_{1-3} (acute angles), as illustrated in Figure 4. This broke the geometric symmetry and made n-π* transitions more allowed with remarkably increased *f* of 0.01 – 0.09 (Tables S22 – S24). As a result, *Z*-isomers showed relatively strong n-π* absorbance against *E*-isomers, responsible for quantitative *Z*→*E* photoisomerization.

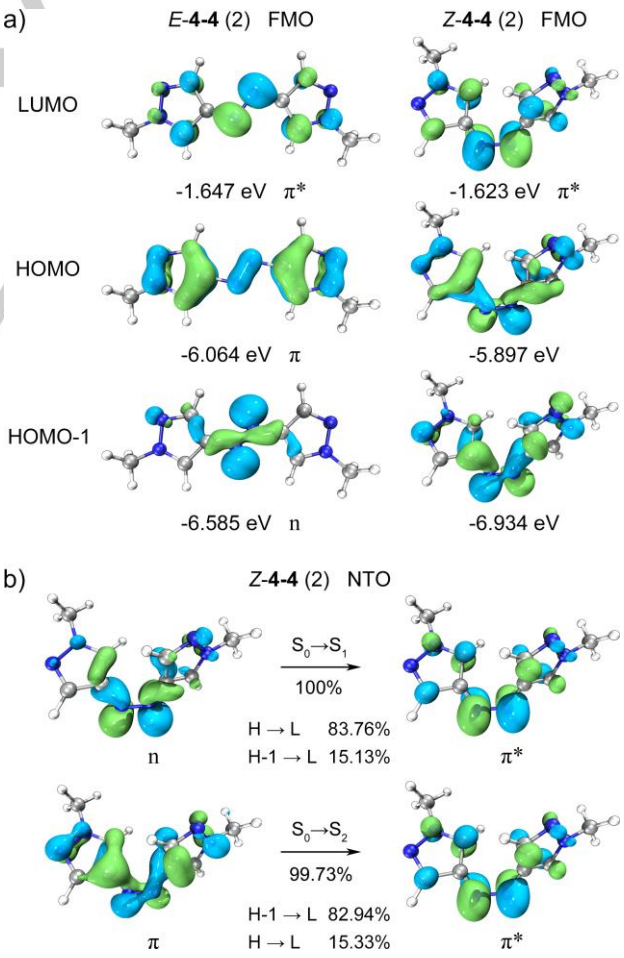

Figure 3. (a) Frontier molecular orbitals and (b) natural transition orbitals for the predominant conformers of **4-4** (isosurface value of 0.05). Results of other molecules were illustrated in Figures S35 – S40.

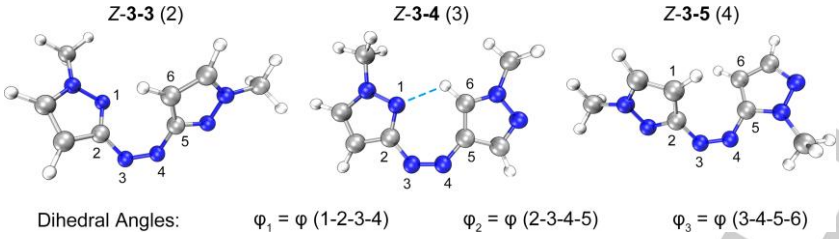

	Z-**3-3**		*Z*-**3-4**		*Z*-**3-5**		*Z*-**4-4**		*Z*-**4-5**		*Z*-**5-5**		*Z*-Azobenzene
Conformation	(2)	(1)	(3)	(4)	(4)	(3)	(2)	(1)	(3)	(1)	(1)	(3)	(*Z*-**Azo**)
Population (%)	60.4	23.5	41.6	30.0	75.0	13.8	64.2	30.7	50.7	24.9	87.8	12.2	100
φ_1 (°)	53.9	39.2	0.0	44.5	25.6	0.0	36.5	32.7	70.9	39.3	13.6	28.8	51.6
φ_2 (°)	9.8	12.0	0.0	9.8	11.2	0.0	9.4	9.9	4.8	10.3	7.2	11.0	9.1
φ_3 (°)	18.6	39.2	0.0	20.3	34.7	0.0	28.6	32.7	7.1	19.3	63.6	28.8	51.6
Avg.(φ_1,φ_3) (°)	36.3	39.2	0.0	32.4	30.2	0.0	32.6	32.7	39.0	29.3	38.6	28.8	51.6

Figure 4. The geometric structure and dihedral angles of *Z*-isomers (optimized at PBE0-D3(BJ)/6-31G** level of theory in MeCN).

Geometric Insight

For the *Z*-isomer geometry, azobispyrazoles are actually in a similar situation with azobenzenes (also twisted) where the two rings and azo group avoid coplanarity due to steric reasons. However, *Z*-azobispyrazoles are less twisted from planar geometry than *Z*-azobenzene (*Z*-**Azo**): as detailed in Figure 4, *Z*-**Azo** is characterized by large φ_1 and φ_3 (both over 50°)[33] while for *Z*-azobispyrazoles at least one of the twist angles is smaller than 30° (averaged values of φ_1 and φ_3: 28 – 40°). This difference indicates that the intramolecular steric hindrance associated with six-membered ring is remarkably weakened by two five-membered rings. This viewpoint can also be understood from an energetic perspective. We calculated the Gibbs free energy difference between the twisted geometry (energy minimum conformation) and a near-planar geometry ($\varphi_1 = \varphi_2 = \varphi_3$ = 10°). As shown in Figure 5a, the energy increase was 190 kJ/mol for *Z*-**Azo** to reach the near-planar geometry, but much lower energy increases of 49 – 101 kJ/mol were found for the series of *Z*-azobispyrazoles.

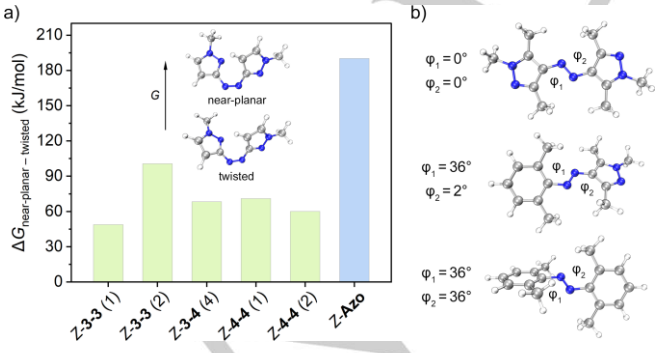

Figure 5. (a) Gibbs free energy difference between normal twisted and restricted near-planar geometries (computed at B2PLYP-D3(BJ)/def2-TZVP//PBE0-D3(BJ)/6-31G** level of theory in MeCN with solvation free energies at M05-2X/6-31G* level). (b) The geometric structure and dihedral angles of *ortho*-tetramethyl azo molecules (optimized at PBE0-D3(BJ)/6-31G** level of theory in MeCN).

Interestingly, a couple of planar conformers were found in *Z*-**3-4** and *Z*-**3-5** ($\varphi_1 = \varphi_2 = \varphi_3 = 0°$), which were stabilized by an intramolecular C–H···N hydrogen bond between the pyridine-type N atom on 3-pyrazole ring and a C–H group on the other ring (Figure 4 and S31). These planar conformers showed small *f* of 0.0018 – 0.0026 (Tables S22 – S24). *Z*-**3-4** had two planar conformers (conformer (1) and (3), see Figure 4 and S31) and their total population accounted for 55% (Boltzmann distribution, see Table S19), explaining its relatively low n-π* band observed in Figure 2, while the absorbance of *Z*-**3-5** was of "normal" intensity because its sole planar conformer (3) was of small distribution (only 14%). Planar *Z*-isomers were never observed in Ph-N=N-Ph or Ph-N=N-Het type molecules but were also found in other five-membered ring based azobisheteroarenes involving C–H···N hydrogen bond, including azobis(2-imidazole),[21] its protonated product,[21] and protonated azobis(benzothiazole).[22] This unique phenomenon shows again that two five-membered rings result in weakened steric hindrance, and it can be overcome by a weak hydrogen bond.

For the *E*-isomers, two five-membered rings provide a more spacious molecular environment to accommodate bulky substituents. This was directly demonstrated using *ortho* methyl as the probing group. As shown in Figure 5b, the introduction of four *ortho* methyl groups to azobenzene forced both phenyl rings to rotate away from coplanarity with the azo group, resulting in a highly twisted geometry. When one of the phenyl rings was replaced by a pyrazole ring, half of the crowdedness was eliminated. By contrast, the azobispyrazole structure was free of any steric perturbation and kept the planar geometry. In this case, the electronic excitation characteristics of the parent molecule were not substantially affected by the bulky methyls (Table S26). It is known that the twisted geometry inevitably interrupts the conjugation of a π-system, which is undesirable in many conditions. Introducing fluorines is the only reported way to maintain the tetra-*ortho*-substituted azobenzene planar, benefiting from the small atomic size.[9c] Azobispyrazole and other Het-N=N-Het molecules may act as a more versatile platform where electronic effect of bulky substituents can also be utilized without affecting the effective conjugation.

Thermal *Z*→*E* Isomerization

The thermal *Z*→*E* isomerization of azobispyrazoles followed first-order kinetics (see Section 3 in SI), and their *Z*-isomer $t_{1/2}$ and thermodynamic activation parameters at 25 °C were listed in Table 1. Very long $t_{1/2}$ of nearly 2 years were achieved by **4-4** and **3-4**, making them rare azo switches possessing highly stable *Z*-isomers.[9c,14a,34] The $t_{1/2}$ could be further regulated to months, weeks, days, and hours by adjusting the linkage pattern. Such a widely tunable $t_{1/2}$ could meet the kinetic requirements of a broad spectrum of photo-responsive systems. We could find that the *Z*-isomer stability did not rely on its geometric shape, since the twisted geometry allowed widely tunable $t_{1/2}$. This was in stark contrast with the structure-property relationship established for mono-heteroaryl molecular system based on imidazole, pyrazole, pyrrole, triazole, and tetrazole, for which the T and twisted shape dictates long and short $t_{1/2}$, respectively.[14b]

A clear trend between *Z*-isomer $t_{1/2}$ and bridging position was found: 4-pyrazole unit favored long $t_{1/2}$ the most, followed by the 3-pyrazole and finally the 5-pyrazole, and $t_{1/2}$ took orders from the combination of the two units, i.e., **4-4** > **3-4** > **3-3** > **4-5** > **3-5** > **5-5**. In order to understand the thermal *Z*→*E* isomerization behavior of azobispyrazole family, we studied their isomerization processes via rotation and inversion by relaxed potential energy scans, as depicted in Figure 6a. Our results suggested that the lowest energy pathway followed the rotational mechanism, instead of the inversion mechanism found for mono-pyrazolyl azo switches.[14b] Based on the computed Gibbs free energies of *Z*-isomers and transition states (G_Z and G_{TS}), theoretical free energy barriers ($\Delta G^{\ddagger}$) were obtained (Table 1 and S21), which were well correlated with the experimental values, as illustrated in Figure 6b.

Since G_{TS} and G_Z were influenced by intramolecular stabilizing/destabilizing interactions, the noncovalent interaction (NCI) analysis[32,35] of transition states (TSs) and *Z*-isomers was performed. The results of their predominant conformers were shown in Figure 6c. For the TSs of the molecules with 5-pyrazole (**4-5**, **3-5**, and **5-5**), the bulky *N*-methyl on 5-pyrazole were adjacent to the azo group, enabling them to form dispersive interactions, while such stabilizing interactions were absent for the other three molecules (their *N*-methyls were away from azo groups). Therefore, it was easier for the 5-pyrazole series to overcome the energy barriers. For the *Z*-isomers of this series, the *N*-methyl group on 5-pyrazole of **4-5** orientated towards the side of the remaining azo-pyrazolyl part; it gave rise to the largest dispersive surface that stabilized *Z*-**4-5** the most,

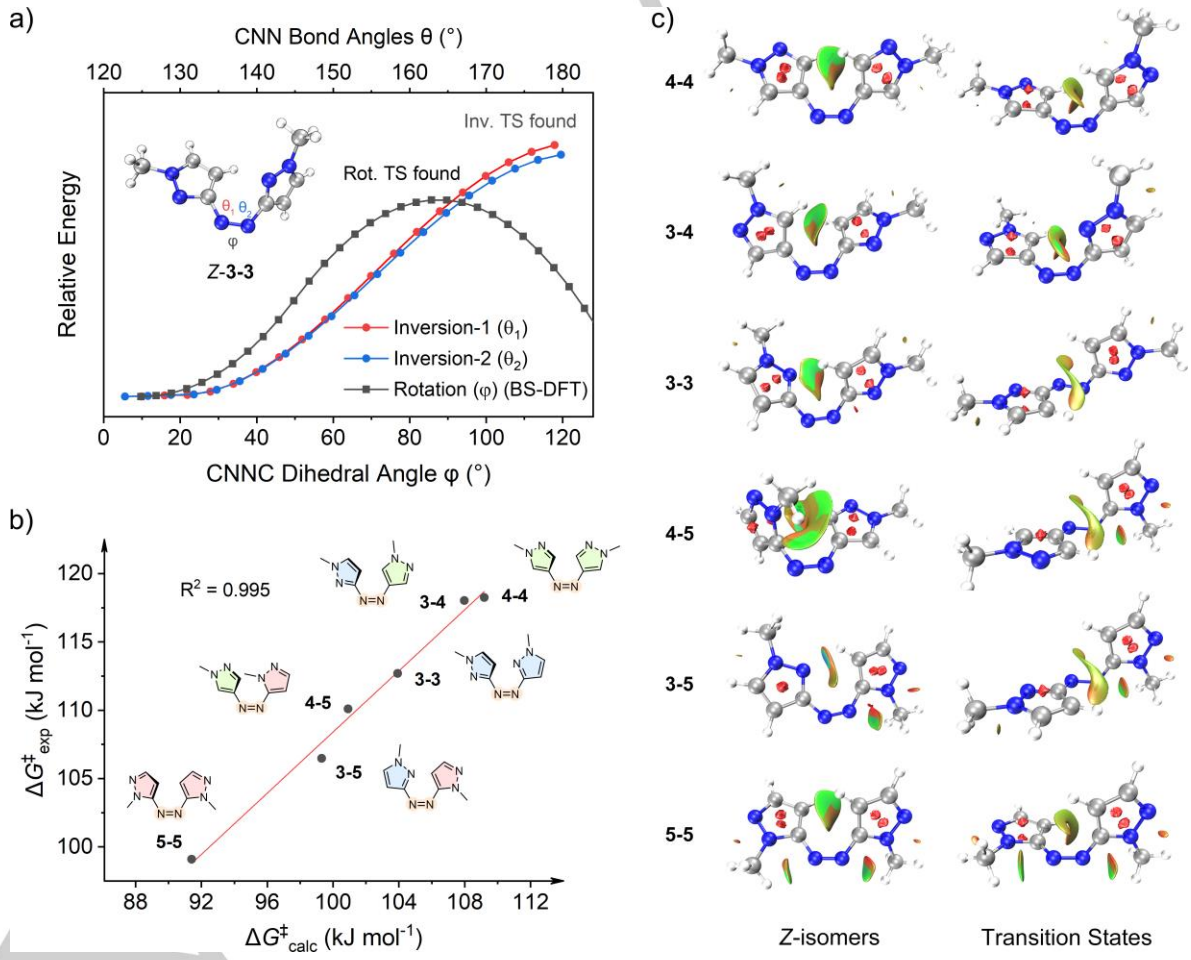

Figure 6. (a) Typical relaxed potential energy scans of the thermal *Z*→*E* isomerization of azobispyrazoles in DMSO (taking **3-3** as an example) at PBE0-D3(BJ)/6-31G** level of theory (using broken symmetry (BS) approach for rotational pathway). (b) Linear correlation between experimental and computed free energy barriers for azobispyrazoles in DMSO. (c) NCI surfaces of the predominant *Z*-isomers and transition states for azobispyrazoles in DMSO (isosurface value of 0.75). The surfaces were colored on a blue-green-red scale according to the values of sign(λ_2)·ρ, ranging from -0.04 to 0.02 au.[35]

explaining its longest $t_{1/2}$ in this series. The higher stability of *Z*-**3-5** than *Z*-**5-5** was probably attributed to the relatively stronger stabilizing effect of intramolecular C–H···N hydrogen bond in planar *Z*-**3-5**. For the other three molecules (**4-4**, **3-4**, and **3-3**), their *Z*-isomers displayed similar NCI surfaces, and their TSs faced the same situation, which made it difficult to qualify the difference in their energy barriers through NCI pictures. Indeed, $\Delta G^{\ddagger}$ of their considered conformers were only slightly different ($\Delta G^{\ddagger}_{4\text{-}4} - \Delta G^{\ddagger}_{3\text{-}4}$ = 1.0 kJ/mol, $\Delta G^{\ddagger}_{3\text{-}4} - \Delta G^{\ddagger}_{3\text{-}3}$ = 2.6 kJ/mol). Interestingly, for the TSs, a dispersive interaction between the *N*-methyl and adjacent C–H group on 3-pyrazole was observed, whereas this interaction on 4-pyrazole was negligible. This might contribute to the lower $\Delta G^{\ddagger}$ of the molecules with more 3-pyrazole units.

Conclusion

In conclusion, we have designed and investigated a family of azobispyrazoles as new bis-heteroaryl azo photoswitches. All six members show excellent bidirectional $E \leftrightarrows Z$ photoconversion, and their *Z*-isomer $t_{1/2}$ cover a wide range of timescales including years, months, weeks, days, and hours. Azobispyrazole system bearing 5-pyrazole moiety shows higher π-conjugation, so the π-π* λ_{max} of *E*-isomer follows the order of **5-5** > **3**(**4**)**-5** > **3**(**4**)**-3**(**4**). **5-5** can be used as a bidirectionally visible-light-activated photoswitch. The linkage pattern also directs the thermal back-isomerization kinetics, and $t_{1/2}$ follow the order of **4-4** > **3-4** > **3-3** > **4-5** > **3-5** > **5-5**. This can be explained by the different intramolecular stabilizing interactions brought by 4-, 3-, 5-pyrazole units in TSs and *Z*-isomers.

We reveal that the two five-membered rings on Het-N=N-Het architecture can remarkably weaken the intramolecular steric hindrance compared with phenyl ring(s) on Ph-N=N-Ph and Ph-N=N-Het. This brings new possibilities for engineering the geometric and electronic structure of azo photoswitches. *Z*-azobispyrazoles generally adopt a twisted geometry, which favors n-π* absorption strength and facilitates complete *Z*→*E* photoisomerization. Moreover, the twisted *Z*-isomers provide widely tunable thermal $t_{1/2}$ without compromising the photoisomerization yields. This overcomes the inherent conflict between effective *Z*→*E* photoisomerization (favored by twisted shape) and *Z*-isomer stability (favored by T shape) that exists in the Ph-N=N-Het class based on five-membered *N*-heterocycles (imidazole, pyrazole, pyrrole, triazole, and tetrazole). Therefore, azobispyrazoles show great potential in developing high-performance photocontrollable systems and can inspire the rational design of new photoswitches making use of Het-N=N-Het architecture.

Acknowledgements

This work was supported by the National Key Research and Development Program of China (2017YFA0207500), National Natural Science Foundation of China (22022507, 51973111), Beijing National Laboratory for Molecular Sciences (BNLMS202004) and China Postdoctoral Science Foundation (2020M681279). We acknowledge the Instrumental Analysis Center of Shanghai Jiao Tong University, especially the help of Dr. Lingling Li for single-crystal XRD analysis.

Conflict of interest

The authors declare no competing financial interest.

Keywords: azobenzene • heterocycle • molecular photoswitch • photoisomerization • pyrazole

[1] a) W. Szymański, J. M. Beierle, H. A. V. Kistemaker, W. A. Velema, B. L. Feringa, *Chem. Rev.* **2013**, *113*, 6114-6178; b) K. Glusac, *Nat. Chem.* **2016**, *8*, 734-735; c) M. Baroncini, S. Silvi, A. Credi, *Chem. Rev.* **2020**, *120*, 200-268; d) M. Kathan, S. Hecht, *Chem. Soc. Rev.* **2017**, *46*, 5536-5550; e) J. Zhang, Q. Zou, H. Tian, *Adv. Mater.* **2013**, *25*, 378-399; f) A. Goulet-Hanssens, F. Eisenreich, S. Hecht, *Adv. Mater.* **2020**, *32*, 1905966; g) L. Wang, Q. Li, *Chem. Soc. Rev.* **2018**, *47*, 1044-1097; h) X. Huang, T. Li, *J. Mater. Chem. C* **2020**, *8*, 821-848; i) C. Sun, C. Wang, R. Boulatov, *ChemPhotoChem* **2019**, *3*, 268-283; j) W. Xu, S. Sun, S. Wu, *Angew. Chem. Int. Ed.* **2019**, *58*, 9712-9740.

[2] a) A. H. Gelebart, D. Jan Mulder, M. Varga, A. Konya, G. Vantomme, E. W. Meijer, R. L. B. Selinger, D. J. Broer, *Nature* **2017**, *546*, 632-636; b) T. Ube, T. Ikeda, *Angew. Chem. Int. Ed.* **2014**, *53*, 10290-10299.

[3] a) J. Broichhagen, J. A. Frank, D. Trauner, *Accounts Chem. Res.* **2015**, *48*, 1947-1960; b) F. Riefolo, C. Matera, A. Garrido-Charles, A. M. J. Gomila, R. Sortino, L. Agnetta, E. Claro, R. Masgrau, U. Holzgrabe, M. Batlle, M. Decker, E. Guasch, P. Gorostiza, *J. Am. Chem. Soc.* **2019**, *141*, 7628-7636.

[4] a) L. Dong, Y. Feng, L. Wang, W. Feng, *Chem. Soc. Rev.* **2018**, *47*, 7339-7368; b) S. Wu, H. J. Butt, *Macromol. Rapid Comm.* **2020**, *41*, 1900413; c) Z. Zhang, Y. He, Z. Wang, J. Xu, M. Xie, P. Tao, D. Ji, K. Moth-Poulsen, T. Li, *J. Am. Chem. Soc.* **2020**, *142*, 12256-12264; d) Z. Wang, R. Losantos, D. Sampedro, M. Morikawa, K. Börjesson, N. Kimizuka, K. Moth-Poulsen, *J. Mater. Chem. A* **2019**, *7*, 15042-15047.

[5] a) W. Lin, M. Tsai, R. Rajappa, R. H. Kramer, *J. Am. Chem. Soc.* **2018**, *140*, 7445-7448; b) R. J. Mart, R. K. Allemann, *Chem. Commun.* **2016**, *52*, 12262-12277.

[6] S. Hvilsted, C. Sánchez, R. Alcalá, *J. Mater. Chem.* **2009**, *19*, 6641-6648.

[7] G. S. Hartley, *Nature* **1937**, *140*, 281.

[8] a) H. M. D. Bandara, S. C. Burdette, *Chem. Soc. Rev.* **2012**, *41*, 1809-1825; b) E. Merino, *Chem. Soc. Rev.* **2011**, *40*, 3835-3853.

[9] a) O. Sadovski, A. A. Beharry, F. Zhang, G. A. Woolley, *Angew. Chem. Int. Ed.* **2009**, *48*, 1484-1486; b) A. A. Beharry, O. Sadovski, G. A. Woolley, *J. Am. Chem. Soc.* **2011**, *133*, 19684-19687; c) D. Bléger, J. Schwarz, A. M. Brouwer, S. Hecht, *J. Am. Chem. Soc.* **2012**, *134*, 20597-20600; d) H. A. Wegner, *Angew. Chem. Int. Ed.* **2012**, *51*, 4787-4788; e) S. Samanta, T. M. McCormick, S. K. Schmidt, D. S. Seferos, G. A. Woolley, *Chem. Commun.* **2013**, *49*, 10314-10316; f) M. Dong, A. Babalhavaeji, S. Samanta, A. A. Beharry, G. A. Woolley, *Accounts Chem. Res.* **2015**, *48*, 2662-2670; g) M. J. Hansen, M. M. Lerch, W. Szymanski, B. L. Feringa, *Angew. Chem. Int. Ed.* **2016**, *55*, 13514-13518; h) L. N. Lameijer, S. Budzak, N. A. Simeth, M. J. Hansen, B. L. Feringa, D. Jacquemin, W. Szymanski, *Angew. Chem. Int. Ed.* **2020**, *59*, 21663-21670.

[10] S. Crespi, N. A. Simeth, B. König, *Nature Reviews Chemistry* **2019**, *3*, 133-146.

[11] a) Y. Wang, X. Ge, G. Schull, R. Berndt, H. Tang, C. Bornholdt, F. Koehler, R. Herges, *J. Am. Chem. Soc.* **2010**, *132*, 1196-1197; b) S. Venkataramani, U. Jana, M. Dommaschk, F. D. Sönnichsen, F. Tuczek, R. Herges, *Science* **2011**, *331*, 445.

[12] a) E. Procházková, L. Čechová, J. Kind, Z. Janeba, C. M. Thiele, M. Dračínský, *Chem. Eur. J.* **2018**, *24*, 492-498; b) Y. Xu, C. Gao, J. Andréasson, M. Grøtli, *Org. Lett.* **2018**, *20*, 4875-4879.

[13] a) J. Otsuki, K. Suwa, K. K. Sarker, C. Sinha, *J. Phys. Chem. A* **2007**, *111*, 1403-1409; b) T. Wendler, C. Schütt, C. Näther, R. Herges, *J. Org. Chem.* **2012**, *77*, 3284-3287.

[14] a) C. E. Weston, R. D. Richardson, P. R. Haycock, A. J. P. White, M. J. Fuchter, *J. Am. Chem. Soc.* **2014**, *136*, 11878-11881; b) J. Calbo, C. E. Weston, A. J. P. White, H. S. Rzepa, J. Contreras-García, M. J. Fuchter, *J. Am. Chem. Soc.* **2017**, *139*, 1261-1274.

[15] a) C. Slavov, C. Yang, A. H. Heindl, H. A. Wegner, A. Dreuw, J. Wachtveitl, *Angew. Chem. Int. Ed.* **2020**, *59*, 380-387; b) A. H. Heindl, H. A. Wegner, *Chem. Eur. J.* **2020**, *26*, 13730-13737.

[16] P. Kumar, A. Srivastava, C. Sah, S. Devi, S. Venkataramani, *Chem. Eur. J.* **2019**, *25*, 11924-11932.

[17] a) S. Devi, M. Saraswat, S. Grewal, S. Venkataramani, *J. Org. Chem.* **2018**, *83*, 4307-4322; b) L. Stricker, M. Böckmann, T. M. Kirse, N. L. Doltsinis, B. J. Ravoo, *Chem. Eur. J.* **2018**, *24*, 8639-8647; c) Z. Y. Zhang, Y. He, Y. Zhou, C. Yu, L. Han, T. Li, *Chem. Eur. J.* **2019**, *25*, 13402-13410.

[18] a) N. A. Simeth, S. Crespi, M. Fagnoni, B. König, *J. Am. Chem. Soc.* **2018**, *140*, 2940-2946; b) N. A. Simeth, A. Bellisario, S. Crespi, M. Fagnoni, B. König, *J. Org. Chem.* **2019**, *84*, 6565-6575.

[19] R. Travieso-Puente, S. Budzak, J. Chen, P. Stacko, J. T. B. H. Jastrzebski, D. Jacquemin, E. Otten, *J. Am. Chem. Soc.* **2017**, *139*, 3328-3331.

[20] D. Kolarski, W. Szymanski, B. L. Feringa, *Org. Lett.* **2017**, *19*, 5090-5093.

[21] C. E. Weston, R. D. Richardson, M. J. Fuchter, *Chem. Commun.* **2016**, *52*, 4521-4524.

[22] A. D. W. Kennedy, I. Sandler, J. Andréasson, J. Ho, J. E. Beves, *Chem. Eur. J.* **2020**, *26*, 1103-1110.

[23] P. R. Huddleston, V. V. Volkov, C. C. Perry, *Phys. Chem. Chem. Phys.* **2019**, *21*, 1344-1353.

[24] a) M. M. M. Raposo, A. M. C. Fonseca, M. C. R. Castro, M. Belsley, M. F. S. Cardoso, L. M. Carvalho, P. J. Coelho, *Dyes Pigm.* **2011**, *91*, 62-73; b) P. J. Coelho, M. C. R. Castro, A. M. C. Fonseca, M. M. M. Raposo, *Dyes Pigm.* **2012**, *92*, 745-748; c) P. J. Coelho, M. C. R. Castro, S. S. M. Fernandes, A. M. C. Fonseca, M. M. M. Raposo, *Tetrahedron Lett.* **2012**, *53*, 4502-4506; d) J. Garcia-Amorós, M. C. R. Castro, P. Coelho, M. M. M. Raposo, D. Velasco, *Chem. Commun.* **2013**, *49*, 11427-11429.

[25] H. V. Patel, K. A. Vyas, S. P. Pandey, P. S. Fernandes, *Synthetic Commun.* **1992**, *22*, 3081-3087.

[26] A. Trivella, S. Coussan, T. Chiavassa, *Synthetic Commun.* **2008**, *38*, 3285-3290.

[27] P. López-Tarifa, G. Sánchez-Sanz, I. Alkorta, J. Elguero, D. Sanz, A. Perona, R. M. Claramunt, *J. Mol. Struct.* **2012**, *1015*, 138-146.

[28] K. Rustler, P. Nitschke, S. Zahnbrecher, J. Zach, S. Crespi, B. König, *J. Org. Chem.* **2020**, *85*, 4079-4088.

[29] a) B. V. Lyalin, V. L. Sigacheva, V. A. Kokorekin, T. Y. Dutova, G. M. Rodionov, V. A. Petrosyan, *Russ. Chem. B.+* **2018**, *67*, 510-516; b) B. V. Lyalin, V. L. Sigacheva, V. A. Kokorekin, V. A. Petrosyan, *Tetrahedron Lett.* **2018**, *59*, 2741-2744.

[30] J. Bredas, *Mater. Horizons* **2014**, *1*, 17-19.

[31] R. L. Martin, *J. Chem. Phys.* **2003**, *118*, 4775-4777.

[32] T. Lu, F. Chen, *J. Comput. Chem.* **2012**, *33*, 580-592.

[33] D. B. Konrad, G. Savasci, L. Allmendinger, D. Trauner, C. Ochsenfeld, A. M. Ali, *J. Am. Chem. Soc.* **2020**, *142*, 6538-6547.

[34] J. Calbo, A. R. Thawani, R. S. L. Gibson, A. J. P. White, M. J. Fuchter, *Beilstein J. Org. Chem.* **2019**, *15*, 2753-2764.

[35] E. R. Johnson, S. Keinan, P. Mori-Sánchez, J. Contreras-García, A. J. Cohen, W. Yang, *J. Am. Chem. Soc.* **2010**, *132*, 6498-6506.

10.1002/anie.202103705

Entry for the Table of Contents

Insert graphic for Table of Contents here.

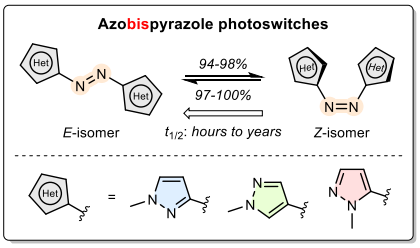

Azobispyrazoles are a family of bis-heteroaryl azo photoswitches that combine excellent *E* ⇆ *Z* photoisomerization yields and widely tunable *Z*-isomer thermal half-lives from hours to years, showing the great potential of Het-N=N-Het architecture in developing high-performance molecular photoswitches.